COMPARISON OF STATIONARY AND TRANSIENT SIMULATIONS OF A LATENT THERMAL ENERGY STORAGE UNIT IN A CARNOT BATTERY

Lauritz Zendel[1]*, Josefine Koksharov[1], Frank Dammel[1], Peter Stephan[1]

[1]Institute for Technical Thermodynamics, Technical University of Darmstadt, Darmstadt, Germany

*Corresponding Author: zendel@ttd.tu-darmstadt.de

ABSTRACT

The expansion of renewable energies is leading to an increasing fluctuation in electricity generation. Besides established concepts such as pumped hydroelectric energy storage for balancing demand and generation, the so-called Carnot battery (CB) is an emerging technology to store electrical energy. A CB consists of a heat pump, a thermal energy storage unit, and a heat engine. The heat pump is used for the charging process, which converts electrical energy to thermal energy. After storing the thermal energy in the thermal energy storage unit, the heat engine is used to discharge the storage unit and supply electrical energy. As the competition on the electricity market is high, an optimal configuration has to be found to achieve an economically viable CB.

So far, many different CB systems have been investigated using different configurations including different storage units. Latent thermal energy storage (LTES) units are less explored than sensible thermal energy storage units, but they are promising due to their relatively constant operating temperature and high energy densities. Therefore, CBs based on LTES are examined in this study.

The LTES is a component which should be modeled transiently, as the phase change material (PCM) undergoes a phase change during charging and discharging. Within an optimization problem, the time to carry out a transient simulation exceeds the available computing capacity. Therefore, the transient behavior must be approximated by a stationary simulation. The deviation between stationary and transient results must be quantified in order to assess the uncertainty.

This study investigates the difference between two stationary simulations of a CB based on an LTES unit with erythritol as PCM and the results of a transient simulation of this configuration. The simulations are compared with regard to the coefficient of performance, the efficiency of the heat engine, and the round-trip efficiency. It turns out that both stationary simulations are not capable to approximate the transient simulation satisfactorily. Therefore, the use of several stationary simulations instead of just one stationary simulation could be investigated in the future to achieve the desired objective. For all simulations the commercial software EBSILON®Professional is used.

1 INTRODUCTION

The expansion of renewable energies is a key component in achieving the reduction of CO_2 emissions for each country (COP28, IRENA, GRA (2023)). However, due to their dependence on weather conditions the energy supply from renewable energies is subject to fluctuations. To reconcile the electricity consumption and demand, energy storage represents one possible solution. Next to well-established technologies such as pumped hydroelectric energy storage the so-called Carnot battery (CB) can be a future option. A CB consists of a heat pump (HP), which converts electrical energy in thermal energy during the charging process. The thermal energy is stored in a thermal energy storage unit. For the discharging process a heat engine (HE) is applied to transform the thermal energy into electrical energy. In this study, CBs with latent thermal energy storage (LTES) units are investigated. LTES units are based on phase change materials (PCMs) and therefore allow the storage of thermal energy in a narrow temperature range. This is advantageous for the combination with a Rankine cycle, in which evaporation of the heat transfer fluid (HTF) at a constant temperature takes place. Compared to sensible thermal energy storage units, LTES units are less developed (Scheffler (2019)) and therefore subject of

https://doi.org/10.52202/077185-0036

research. As the PCM in an LTES is subject to a phase change during both during the charging and discharging process, transient simulations are carried out to capture this.

Many studies in the field of LTES consider its transient behavior to investigate different aspects. Arena *et al.* (2018) numerically studied the influence of a partial load operation of an LTES. For this purpose, four charging and subsequent discharging processes with different melting fractions were simulated for a lab-scale vertical concentric tube without fins. A complete melting corresponds to a melting fraction of 1 representing the base case. Additionally, melting fractions 0.95, 0.90 and 0.75 were considered. It turned out that the reduction of the prescribed melting fraction down to 0.75 requires half of the time for the charging process compared to the base case accompanied by 30 % lower energy stored.
Raul *et al.* (2020) performed transient simulations of different configurations of an LTES integrated in a concentrated solar power plant. Investigations regarding the influence of the number and the thickness of the fins inside the storage were carried out analyzing their influence on the melting fraction of the PCM, the power generation of the plant and the discharge efficiency. Tehrani *et al.* (2016) studied the design of an LTES with three PCMs for the application in a concentrated solar thermal tower plant operated in the temperature range from 286 °C to 565 °C. The non-dimensional length, the non-dimensional radius and three different lengths of the storage were investigated. Transient simulations were performed assuming a charging and discharging duration of 10 h each.
In the context of CBs, several studies based on transient simulations are available. Zheng *et al.* (2023) experimentally and numerically studied a rectangular LTES for application in a CB. Besides the reference case a variation in mass flow and HTF temperature was numerically examined using transient simulations. Additionally, the influence of the number and thickness of the fins as well as their material was investigated. The time required for the melting and solidification process is used as a measure to compare the setups. They found that a change in the HTF temperature has a greater effect on the charging and discharging time than a change in mass flow.
Meidinger *et al.* (2018) simulated a CB based on a vertically finned LTES. A single pipe of the LTES was modeled and transiently simulated to approximate the performance of the entire storage unit. The charging and discharging duration amounts to 4 h each. Exergetic, economic and exergoeconomic analyses were performed to assess the system under investigation. A round-trip efficiency of 38 % was determined. Additionally, the high component cost was found to prevent the CB from operating economically.
In the study of Santos *et al.* (2023) economic aspects of a CB are investigated with a transient Matlab model. A CB which makes use of the heat of a solar thermal panel and electricity from a PV array during the charging process stores thermal energy in a sensible thermal energy storage tank. Temperature, and therefore pressure, changes during both charging and discharging. The influence of the pinch points and the storage size as well as the accompanied costs of the heat exchangers and the storage tank are subject of this investigation. A Pareto front which shows a tradeoff between costs and efficiency summarizes the findings of their research.
Another transient Matlab model was developed by Xue and Zhao (2023) to analyze a Brayton cycle-based CB with encapsulated PCM used in both, the hot and cold LTES unit. The focus of the study was to compare two configurations which differed in the use of a recuperator. Among other things, round-trip efficiency and energy density were investigated for different pressure ratios and working fluids. In addition, the spacial temperature distribution, and the temperature distribution over time within the storages were examined. An exergy analysis showed a higher round-trip efficiency for the systems with a recuperator.
Many efforts are also being made to develop simplified models of an LTES. Parry *et al.* (2014) performed simulations for a 3D and a 1D model of a horizontally oriented LTES. Besides a base configuration a system with circular and longitudinal fins was examined. Additionally, four tubes were considered instead of a single tube. For the mentioned configurations the thermal conductivity of the PCM domain in the 1D model was scaled to obtain a good agreement with the 3D model. Comparing both models, the CPU times could be reduced by four orders of magnitude retaining an acceptable level of accuracy regarding average PCM temperature predictions and heat transfer rates.
Waser *et al.* (2018) developed a 1D model of a salt hydrate based LTES. The validated model shows good agreement with experimental data regarding the HTF outlet temperature. Additionally, employing

https://doi.org/10.52202/077185-0036

an analytical model to determine the effective thermal conductivity of the fin and tube heat exchanger in the LTES enables to use the model without further calibration for deviating materials and geometries. The model can be used for annual simulations, as the course of a day can be calculated in less than 3s. Both, Parry *et al.* (2014) and Waser *et al.* (2018) apply an effective thermal conductivity to take the influence of the fins and neglected physics, e.g. natural convection, into account.
A study of a CB based on the simplification of modeling an LTES as a constant temperature level was carried out by Jockenhöfer *et al.* (2018) with the software EBSILON®Professional. The thermal energy is assumed to be stored in a sensible and a latent thermal energy storage unit. The LTES unit was modeled as a condenser during charging and as a heat exchanger during discharging. The charge-dependent temperature of the LTES unit and thus its time dependence was not considered. Different source and sink temperatures were analyzed to investigate the applicability of a CB for sector coupling. An exergy analysis concludes the investigation.
However, no comparison of stationary and transient simulations for LTES units was found in the literature. Román and Hensel (2022) examined a solar air heater system and compared results obtained by a transient simulation with a temporal resolution of 2s with a stationary simulation which is based on a temporal resolution of 1h. They found that the stationary model predicts a lower energy output of the system than the transient model does, especially for fluctuating weather conditions. The authors therefore conclude that a transient model should be used if there is a downstream process that is sensitive to temperature variations, such as an LTES. The output temperature as well as the energy output of a solar air heater is subject to external influences (weather conditions), which represents a significant difference to the system under consideration and prevents the transfer of the conclusions.
Thus, to the best of the authors knowledge, no study is available to estimate the performance of a CB with an LTES based on a stationary simulation compared to a transient simulation. It is necessary to evaluate the influence of the simplification made by a stationary approach, for example, for a CB system optimization where a transient simulation is not feasible in terms of time.

To fill this research gap in the field of CBs the present study deals with that topic. The coefficient of performance (COP) of the HP, the efficiency of the HE as well as the round-trip efficiency of the CB are used to compare two stationary simulations with the results of a transient simulation.

2 SYSTEM DESIGN

The investigated design of the CB corresponds to the system of Meidinger *et al.* (2018). Their system has a nominal electrical input power of 15 MW. It consists of a HP process, an LTES, and a HE process. Both the HP and the HE are equipped with an internal heat exchanger and butane is used as working fluid. Erythritol is applied as PCM. The results of the transient simulation by Meidinger *et al.* (2018) are compared to two stationary setups, where the LTES is represented by heat exchangers. The structure of these setups is explained in the following.

The schematic of the stationary HP process with the different states at the inlet and outlet of each component can be seen in figure 1. During the HP process the working fluid transfers heat to the LTES by condensation (HP 1 – HP 2). Passing the internal heat exchanger, the working fluid is cooled down (HP 2 – HP 3) and warms up the opposite side (HP 5 – HP 6). After the pressure reduction in a throttle valve (HP 3 – HP 4), the working fluid absorbs heat and evaporates in the evaporator by extracting heat from a heat source, e.g. a river (HP 4 – HP 5). Downstream of the internal heat exchanger the pressure of the working fluid is increased by the compressor (HP 6 – HP 1) and again reaches the initial state.

https://doi.org/10.52202/077185-0036

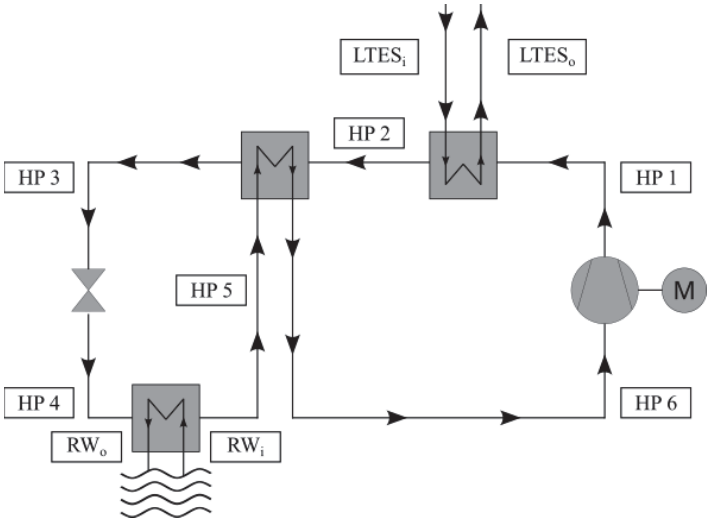

Figure 1: Structure of the stationary HP process.

The stationary HE process with the different states at the inlet and outlet of each component is depicted in figure 2. In the HE process the working fluid passes the turbine and is thereby cooled down (HE 1 – HE 2). Afterwards, heat is transferred in the internal heat exchanger (HE 2 – HE 3) and the working fluid condenses in the condenser by releasing heat to a heat sink, e.g. a river (HE 3 – HE 4). The liquid working fluid is compressed in the pump (HE 4 – HE 5) and preheated in the internal heat exchanger (HE 5 – HE 6). Finally, heat from the LTES is absorbed while the working fluid evaporates (HE 6 – HE 1) and the cycle is closed.

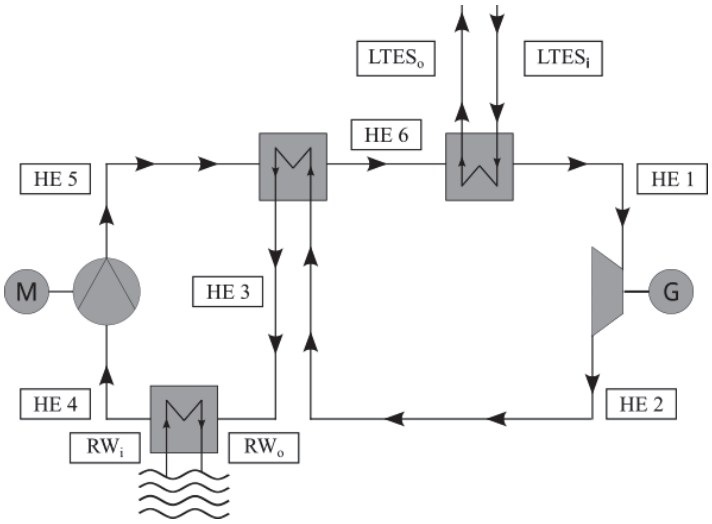

Figure 2: Structure of the stationary HE process.

https://doi.org/10.52202/077185-0036

3 MODELING APPROACH

Two stationary simulations are carried out and compared with the transient case. The average electrical input power was calculated on the basis of the transient simulation results, on which the study by Meidinger *et al.* (2018) is also based. It amounts to 11.558 MW. The stationary simulations are designed with this power for reasons of comparison, even though the thermodynamic states in the stationary simulation do not depend on the electrical input power of the system. Instead, the mass flow depends on the electrical input power.

The first setup is called *Melting Point* (MP) setup. The MP setup is characterized by the design of the HP and HE process based on the melting point of the PCM used in the LTES. For this setup no prior knowledge of the results of a transient simulation is needed. Therefore, an approximation of the transient behavior by that setup would enable significant time savings.
The *Design Point* (DP) setup is defined by the average states during the transient simulation, which could form the basis for designing the components within the HP and HE process. This setup presupposes that the design points are known.

Table 1: Components used and nominal values of their parameters.

Component	Parameter	Value	Ebsilon component number
HP compressor	η_{is}	80 %	24
	η_{mech}	99 %	
HP compressor motor	η_{elec}	96.2 %	29
	η_{mech}	99.8 %	
HE turbine	η_{is}	85 %	6
	η_{mech}	99.8 %	
HE turbine generator	η_{gen}	96.2 %	11
HE pump	η_{is}	80 %	8
	η_{mech}	99.8 %	
HE pump motor	η_{elec}	96.2 %	29
	η_{mech}	99.8 %	

Table 2: Heat exchangers used.

HP	Ebsilon component number	HE	Ebsilon component number
HP evaporator	26	HE evaporator	26
HP internal heat exchanger	26	HE internal heat exchanger	26
HP condenser	7	HE condenser	7
HP subcooler (DP setup only)	26		

The simulations within this study are carried out with the software EBSILON®Professional (Ebsilon) (Iqony Solutions GmbH (2023)). Standard components are available and can be parametrized and connected with the aid of a graphical user interface. Additionally, components can be modified by the user (Iqony Solutions GmbH (2023)). All components used for the modeling are standard components available in Ebsilon and listed in tables 1 and 2. The Ebsilon component number, which is a unique identifier for each component, is specified. Furthermore, the main parameters and their corresponding values are shown in table 1. No pressure drop is assumed in the heat exchangers. Heat losses of the

https://doi.org/10.52202/077185-0036

components and the LTES remain unconsidered. The influence of the pipes between the components regarding pressure drops and heat losses is also neglected.

The parameters of the MP setup and the DP setup are given in tables 3 and 4. According to Agyenim *et al.* (2011), the melting point of erythritol, which is the basis for the MP setup, is assumed to be 117.7 °C. The pressure in the MP setup is set in such a way that the evaporation temperature of the HTF is 5 K below the outlet river water temperature of 9 °C (RW_o in figure 1) and 5 K above the outlet LTES temperature of 117.7 °C ($LTES_o$ in figure 1) in the HP. In the HE, the evaporation temperature of the HTF is 5 K below the outlet LTES temperature of 117.7 °C ($LTES_o$ in figure 2) and 5 K above the outlet river water temperature of 11 °C (RW_o in figure 2). This ensures a pinch point of 5 K. The internal heat exchanger of the HP has an upper terminal temperature difference of 5 K, whereas a lower terminal temperature difference of 5 K is applied to the internal heat exchanger of the HE.

Table 3: Parameters of the MP setup and DP setup of the HP. Fluid properties from Huber *et al.* (2018), Bücker and Wagner (2006).

State	HP 1	HP 2	HP 3	HP 4	HP 5	HP 6
p_{MP} in bar	23.21	23.21	23.21	1.20	1.20	1.20
T_{MP} in °C	223.9	122.7	50.2	4.0	5.0	117.7
p_{DP} in bar	16.80	16.80	16.80	1.19	1.19	1.19
T_{DP} in °C	136.0	71.8	49.4	3.8	7.2	41.5

Table 4: Parameters of the MP setup and DP setup of the HE. Fluid properties from Huber *et al.* (2018), Bücker and Wagner (2006).

State	HE 1	HE 2	HE 3	HE 4	HE 5	HE 6
p_{MP} in bar	19.40	1.82	1.82	1.82	19.40	19.40
T_{MP} in °C	112.7	40.1	22.0	16.0	17.0	30.4
p_{DP} in bar	13.83	1.66	1.66	1.66	13.83	13.83
T_{DP} in °C	129.3	72.4	17.6	13.2	13.9	54.3

For the DP setup the simulation results from Meidinger *et al.* (2018) are used. The average values in the HP and HE for the cyclic steady-state behavior are calculated based on the simulation results and can be seen in tables 5 and 6. The temperature and the pressure values in the states are used to define the states of the HP and HE process.
The average values do not result in a stationary simulation. This is due to the fact, that the system is nonlinear. By averaging the temperatures and pressures this aspect is not considered and consequently deviations between the calculated values and the states in the DP setup have to be tolerated. The states upstream and downstream the condensers and evaporators were prioritized over the states before the valve and compressor in the HP (HP 3, HP 6) and after the turbine and the pump in the HE (HE 2, HE 5). Unlike in the MP setup, a subcooler is used in addition to the condenser in the HP, as the working fluid must be subcooled to achieve the desired temperature at the specified pressure. No additional superheater in the HE is necessary because the component used to model the evaporation is capable to superheat the working fluid.

Table 5: Average values of the transient simulation of the HP based on the simulation results of Meidinger *et al.* (2018).

State	HP 1	HP 2	HP 3	HP 4	HP 5	HP 6
p_{av} in bar	16.80	16.08	16.03	1.24	1.06	1.02
T_{av} in °C	136.0	71.8	56.0	5.0	7.2	32.3

https://doi.org/10.52202/077185-0036

Table 6: Average values of the transient simulation of the HE based on the simulation results of Meidinger *et al.* (2018).

State	HE 1	HE 2	HE 3	HE 4	HE 5	HE 6
p_{av} in bar	13.00	1.85	1.76	1.66	13.92	13.83
T_{av} in °C	129.3	77.0	17.6	13.2	13.9	57.8

The temperature-entropy diagrams of the MP setup, the DP setup and the average values of the transient simulation can be seen in figure 3. Temperatures higher than the melting point of the PCM in the HE (HE 1) are reasonable because the temperature of the PCM regionally exceeds its melting point after the phase change has taken place and additional sensible heat is stored during the HP process. The similarity between the DP setup and the average values becomes apparent. The states of the MP setup deviate clearly. Neither subcooling in the HP process nor superheating in the HE process take place. Additionally, the higher temperature after the compressor represents a substantial difference.

The simulations are compared with respect to their COP, efficiency of the HE (η_{HE}) and round-trip efficiency (η_{rt}). The COP is defined as

$$COP = \frac{\dot{Q}_{\mathrm{LTES,HP}}}{P_{\mathrm{in}}}, \tag{1}$$

where $\dot{Q}_{\mathrm{LTES,HP}}$ is the heat flow transferred to the LTES, and P_{in} is the electric power to drive the motors necessary to operate the HP. The efficiency of the HE η_{HE} is calculated according to

$$\eta_{\mathrm{HE}} = \frac{P_{out}}{\dot{Q}_{\mathrm{LTES,HE}}}, \tag{2}$$

where P_{out} is the electric output power of the HE, which is composed of the electric power output of the generator and the electric power input of the motors used in the HE. $\dot{Q}_{\mathrm{LTES,HE}}$ represents the heat flow removed from the LTES. The round-trip efficiency η_{rt} is defined as the product of the COP and η_{HE}. In a stationary approach, $\dot{Q}_{\mathrm{LTES,HP}}$ and $\dot{Q}_{\mathrm{LTES,HE}}$ are identical, which is why the following formula results:

$$\eta_{\mathrm{rt}} = COP \cdot \eta_{\mathrm{HE}} = \frac{P_{\mathrm{out}}}{P_{\mathrm{in}}}. \tag{3}$$

https://doi.org/10.52202/077185-0036

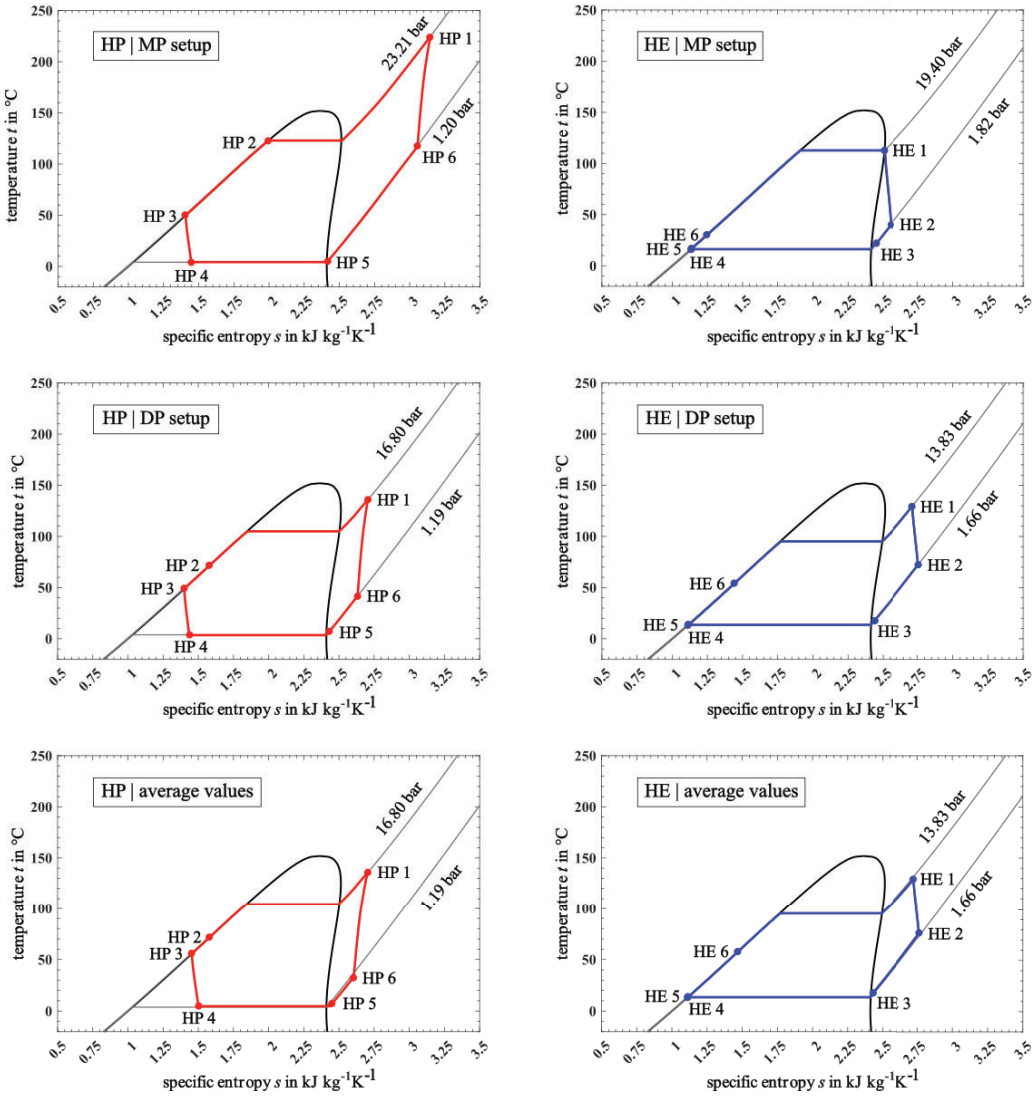

Figure 3: T,s-diagrams of the MP setup (top), DP setup (middle) and the average values of the transient simulation (bottom) for the HP process (left column) and the HE process (right column).

4 RESULTS AND DISCUSSION

The COPs, the efficiencies of the HE and the round-trip efficiencies of the two stationary simulations as well as the one from the transient simulation conducted by Meidinger *et al.* (2018) are depicted in table 7. The COPs of the three simulations differ significantly in terms of relative values. While the MP setup underestimates the COP, the DP setup overestimates it. The efficiency of the HE has lower relative deviations. The MP setup shows a good agreement with the transient case, while the DP setup exhibits a greater deviation. Regarding the round-trip efficiency, it becomes clear, that the MP setup has a smaller deviation than the simulation based on the design points. Even though the absolute discrepancy is only 3.87 %, this corresponds to a relative deviation of 10.1 % compared to the transient case. The DP setup shows a round-trip efficiency which is 7.88 % higher in absolute terms than that of the transient simulation, which corresponds to a relative deviation of more than 20 %. Consequently, both stationary simulations do not properly approximate the performance of the system.

https://doi.org/10.52202/077185-0036

Table 7: COP, η_{HE} and η_{rt} of the simulations.

Parameter	MP setup	DP setup	Transient simulation by Meidinger *et al.* (2018)
COP	2.12 (− 11.7 %)	2.68 (+ 11.7 %)	2.40
η_{HE} in %	16.25 (+ 1.6 %)	17.24 (+ 7.8 %)	15.99
η_{rt} in %	34.50 (− 10.1 %)	46.25 (+ 20.5 %)	38.37

To understand the reasons why both setups show different results compared to the transient case, the enthalpies of the states in the three setups are examined first. It can be seen from figure 4 that the enthalpies between the DP setup and the average values of the transient simulation are almost identical for most states in the HP and HE process. The MP setup shows significant deviations especially in the states 1, 2 and 6 in the HP and HE, respectively. These states are the ones associated with the compressor and the turbine as well as with the condenser and evaporator in the HP and HE, respectively, which represent the LTES. Compared to the transient case no subcooling is allowed resulting in a higher temperature after the LTES. To supply the desired power the temperature after the compressor has to be elevated, too. If the temperature at that point is reduced without adding a subcooler, the efficiency of the CB will drop significantly.
Therefore, even though the results of the MP setup seem to be better than those obtained by the DP setup, it has to be regarded as coincidence, because the states in the processes differ too much from the states in the transient setup.

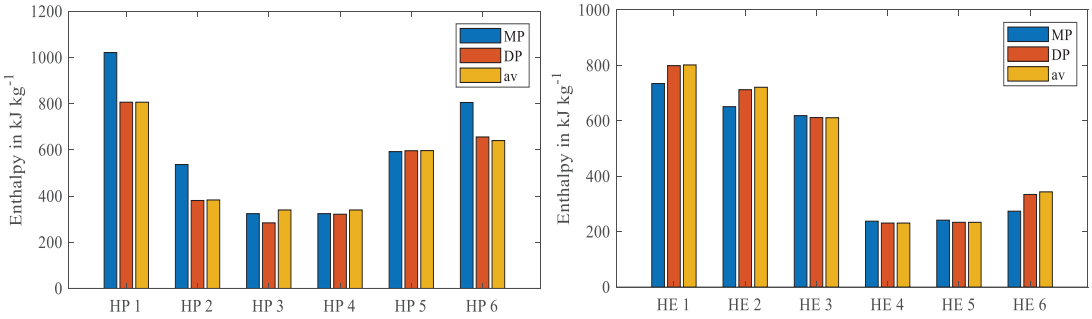

Figure 4: Enthalpies in the HP process (left) and in the HE process (right) of the MP setup, the DP setup and the average values of the transient simulation.

Table 8: Mass flows in the simulations.

Process	MP setup	DP setup	Transient simulation by Meidinger *et al.* (2018)
HP	50.89 kg s^{-1} (− 21.7 %)	72.85 kg s^{-1} (+ 12.1 %)	65 kg s^{-1}
HE	53.27 kg s^{-1} (− 11.2 %)	66.67 kg s^{-1} (+ 11.1 %)	60 kg s^{-1}

The states of the DP setup agree well with the states in the transient simulation (see figure 3). Nevertheless, both the COP and the efficiency of the HE are considerably higher. This is explained by the increased mass flows in the DP setup compared to the transient simulation (see table 8), which is necessary to supply the demanded electric power to the system. The DP setup has a 12.1 % and 11.1 % higher mass flow in the HP and the HE, respectively. Therefore, a higher heat flow to and from the storage can be achieved applying similar states in the processes. Consequently, also the DP setup is not suitable to approximate the transient behavior of the system. Looking at table 8, it is striking that the mass flow in the MP setup is lower in the HP and HE process compared to the transient case. This is

https://doi.org/10.52202/077185-0036

due to the fact, that the difference in enthalpy by transferring heat to and absorbing heat from the storage is larger than that in the transient simulation.

Another fact to keep in mind when comparing the stationary simulations to the transient case is that the transient simulation exhibits significant changes in the thermodynamic states during the simulation. While the temperature before the compressor (HP 6) increases by 24.9 K, the temperature after the compressor (HP 1) increases by 29.6 K. Additionally, the temperatures after the LTES (HP 2) and the internal heat exchanger (HP 3) change by 61.9 K and 49.0 K, respectively. During the HE process, temperature variations of 36.8 K (HE 6), 48.9 K (HE 1), and 52.8 K (HE 2) can be observed. All other states show deviations in temperature of less than 4 K. These differences in the thermodynamic states are accompanied by a varying efficiency over time.

5 CONCLUSION AND OUTLOOK

Based on the results, the following conclusions can be drawn:

- The stationary simulation, which is based on the melting point of the PCM, shows an increased COP and a good agreement with the efficiency of the HE compared to the transient simulation. The round-trip efficiency is therefore also increased. The transient simulation is based on significantly different thermodynamic states, as subcooling and superheating are considered. The closeness of the results should therefore be regarded as coincidental and not an indication of agreement between the models, not even with regard to the efficiency of the HE.

- The stationary simulation based on possible design points of the transient setup shows a good agreement between the thermodynamic states, even though small deviations have to be accepted in order to achieve a stationary setup. That means that it is possible to approximate the average values of the states from the transient simulation using a stationary simulation. However, the stationary simulation results in an increased mass flow. This significantly increases both the COP and the efficiency of the HE, which leads to a higher round-trip efficiency.

- As the stationary simulations of a CB with an LTES show substantial relative deviations with regard to the round-trip efficiency compared to the results of the transient simulation, these stationary simulations cannot be applied for an optimization problem where the round-trip efficiency of a CB should be improved by fractions of a percent.

In future studies the course of the transient simulation could be approximated not only by one but by several stationary simulations. By this approach the transient behavior could be reduced to a stationary behavior, which enables the application in an optimization problem for a standardized profile. For this purpose, different PCMs should be considered to provide a procedure for a wide temperature range. An extended approach of the melting point setup, which takes subcooling into account, could improve the performance of this model and thus represent another topic for future investigations.

NOMENCLATURE

COP	coefficient of performance (-)
P	electrical power (W)
$\dot{Q}$	heat flow (W)
η	efficiency (-)

Subscripts

av	average value of the transient simulation of Meidinger *et al.* (2018)
DP	Design Point
HE	heat engine

https://doi.org/10.52202/077185-0036

HP	heat pump
i	inlet
in	input
LTES	latent thermal energy storage
MP	Melting Point
o	outlet
out	output
rt	round-trip

ACKNOWLEDGEMENT

Funding by the German Research Foundation within the Priority Program 2403: 'Carnot-Batteries: Inverse Design from Markets to Molecules' under project number 525974553 is gratefully acknowledged.

REFERENCES

Agyenim, F., Eames, P., and Smyth, M. (2011) Experimental study on the melting and solidification behaviour of a medium temperature phase change storage material (Erythritol) system augmented with fins to power a LiBr/H2O absorption cooling system. *Renewable Energy*, **36**(1), 108–117.

Arena, S., Casti, E., Gasia, J., Cabeza, L. F., and Cau, G. (2018) Numerical analysis of a latent heat thermal energy storage system under partial load operating conditions. *Renewable Energy*, **128**, 350–361.

Bücker, D. and Wagner, W. (2006) Reference Equations of State for the Thermodynamic Properties of Fluid Phase n-Butane and Isobutane. *Journal of Physical and Chemical Reference Data*, **35**(2), 929–1019.

COP28, IRENA, GRA (2023) *Tripling renewable power and doubling energy efficiency by 2030: Crucial steps towards 1.5°C,* International Renewable Energy Agency, Abu Dhabi.

Huber, M., Harvey, A., Lemmon, E., Hardin, G., Bell, I., and McLinden, M. (2018) *NIST Reference Fluid Thermodynamic and Transport Properties Database (REFPROP) Version 10 - SRD 23,* National Institute of Standards and Technology.

Iqony Solutions GmbH (2023) *EBSILON^{\textregistered}Professional,* Iqony Solutions GmbH, Essen.

Jockenhöfer, H., Steinmann, W.-D., and Bauer, D. (2018) Detailed numerical investigation of a pumped thermal energy storage with low temperature heat integration. *Energy*, **145**, 665–676.

Meidinger, J., Dietrich, A., Dammel, F., and Stephan, P. (2018) Analysis of a Pumped Heat Electricity Storage System with Latent Heat Thermal Energy Storage in *Proceedings of ECOS 2018*, University of Minho, Guimarães, Portugal.

Parry, A. J., Eames, P. C., and Agyenim, F. B. (2014) Modeling of Thermal Energy Storage Shell-and-Tube Heat Exchanger. *Heat Transfer Engineering*, **35**(1), 1–14.

Raul, A., Saha, S. K., and Jain, M. (2020) Transient performance analysis of concentrating solar thermal power plant with finned latent heat thermal energy storage. *Renewable Energy*, **145**, 1957–1971.

Román, F. and Hensel, O. (2022) A comparison of steady-state and transient modelling approaches for the performance prediction of solar air heaters. *Energy Conversion and Management: X*, **16**, 100327.

Santos, M., André, J., Mendes, R., and Ribeiro, J. B. (2023) Thermo-Economic Optimization of a Carnot Battery Under Transient Conditions in *36th International Conference on Efficiency, Cost, Optimization, Simulation and Environmental Impact of Energy Systems (ECOS 2023)*, Smith, J. R. (ed), ECOS 2023, Las Palmas De Gran Canaria, Spain, pp. 2171–2182.

Scheffler, F. (2019) Thermische Energiespeicher – Trends, Entwicklungen und Herausforderungen. *Chemie Ingenieur Technik*, **91**(9), 1219–1228.

https://doi.org/10.52202/077185-0036

Tehrani, S. S. M., Taylor, R. A., Saberi, P., and Diarce, G. (2016) Design and feasibility of high temperature shell and tube latent heat thermal energy storage system for solar thermal power plants. *Renewable Energy*, **96**, 120–136.

Waser, R., Ghani, F., Maranda, S., O'Donovan, T. S., Schuetz, P., Zaglio, M., and Worlitschek, J. (2018) Fast and experimentally validated model of a latent thermal energy storage device for system level simulations. *Applied Energy*, **231**, 116–126.

Xue, X. J. and Zhao, C. Y. (2023) Transient behavior and thermodynamic analysis of Brayton-like pumped-thermal electricity storage based on packed-bed latent heat/cold stores. *Applied Energy*, **329**, 120274.

Zheng, S., Li, S., Li, M., Dai, R., Wei, M., and Tian, R. (2023) Experimental and numerical investigation of a rectangular finned-tube latent heat storage unit for Carnot battery. *Journal of Energy Storage*, **71**, 108092.

https://doi.org/10.52202/077185-0036